ISSN 1063-7834, Physics of the Solid State, 2018, Vol. 60, No. 2, pp. 292–298. © Pleiades Publishing, Ltd., 2018.
Original Russian Text © I.G. Vazhenina, R.S. Iskhakov, L.A. Chekanova, 2018, published in Fizika Tverdogo Tela, 2018, Vol. 60, No. 2, pp. 287–293.

MAGNETISM

Spin-Wave Resonance in Chemically Deposited Fe–Ni Films: Measuring the Spin-Wave Stiffness and Surface Anisotropy Constant

I. G. Vazhenina*, R. S. Iskhakov, and L. A. Chekanova

Kirensky Institute of Physics, Siberian Branch, Russian Academy of Sciences, Krasnoyarsk, 660036 Russia

**e-mail: irina-vazhenina@mail.ru*

Received July 20, 2017

Abstract—Single-layer Fe_xNi_{1-x} thin magnetic films have been investigated by the spin-wave resonance technique in the entire concentration range. The surface anisotropy and exchange stiffness constants for the films with a Ni content from 30 to 80 at % have been measured from the experimental standing spin wave spectra. The surface exchange spin wave penetration depth $\delta_C = 20–30$ nm has been determined from the dependences of the surface anisotropy and exchange coupling constants on the $Fe_{20}Ni_{80}$ film thickness in the range of 250–400 nm.

DOI: 10.1134/S1063783418020294

1. INTRODUCTION

Microwave techniques are widely used in studying the dynamic characteristics of magnetic materials of different classes. The ferromagnetic resonance (FMR) and spin-wave resonance (SWR) techniques are conventionally employed in the measurements of dynamic properties of thin ferromagnetic films [1–4]; powder systems are investigated by the FMR technique [5, 6]. Recently, new objects for employing the microwave techniques have become diluted magnetic semiconductors [7–9] and ferromagnetic metal-insulator nanocomposites (the so-called granular alloys) [10, 11], as well as biological and chemical ferrihydrite nanoparticles [12, 13]. A measured characteristic is the imaginary part of magnetic susceptibility $\chi''(\omega, k)$, whose experimental field or frequency dependence makes it possible to determine the spin-wave stiffness $\eta = 2A/M_S$ and effective magnetization M_{eff} and calculate the exchange coupling constant A.

A decisive requirement for detecting the SWR spectrum of a magnetic film is pinning of the magnetic moment on its surfaces [14, 15]; the quantitative estimation of the degree of pining is determined by the value and sign of the surface anisotropy constant K_S. The latter sometimes allows the K_S values to be directly measured from the SWR spectra.

In most cases, the surface anisotropy constant K_S is determined indirectly via analyzing the magnetization curves [12, 16]. The use of this method suggests introduction of a concept of effective magnetic anisotropy K_{eff}, which is the sum of the bulk (K_V) and surface K_S anisotropies

$$K_{\text{eff}} = K_V + \frac{\alpha K_S}{d}, \quad (1)$$

where d is the size parameter of a sample (film thickness or particle size) and α is the morphological coefficient, which amounts to 2 for a film and 6 for a nanoparticle. In this case, to extract the contribution of each term, it is necessary to measure a series of identical samples, where d is the variable parameter.

The SWR spectrum measured experimentally for an individual sample makes it possible to determine the sign of the surface anisotropy constant and quantitatively measure this parameter for the case $K_S < 0$. At $K_S > 0$, this parameter can be estimated qualitatively [17]. Note that any of the variants $|K_S| \neq 0$ leads to the formation of the SWR spectrum in a film [18–21].

The magnetic film synthesis technique proposed in [22, 23] allows one to purposefully establish the boundary conditions meeting both the $|K_S| \neq 0$ and $K_S < 0$ inequality in thin films. The aim of this study was to investigate the surface anisotropy constant and spin-wave stiffness in the chemically deposited Fe–Ni films as functions of their thickness and composition.

2. EXPERIMENTAL

The authors of [22, 23] experimentally demonstrated the possibility of artificial formation of certain boundary conditions on the surface of a thin ferromagnetic film. The key idea of the authors was to

deposit an additional layer with a thickness from 10 to 30 nm with the effective magnetization different from that of the main layer. Deposition of the additional layer with the magnetization exceeding that of the main layer leads to the establishment of the easy-plane boundary conditions on the film surface and the occurrence of a surface oscillation peak in the SWR spectrum. In this work, we synthesized the additional layer in the form of a thin (~20 nm) film of the Co–P alloy; the main layer was a Fe–Ni ferromagnetic thin film. The samples were synthesized on glass substrates by chemical deposition from the solution of the corresponding salts. Two sample series were studied. The first series was fabricated for studying the dependence of the surface anisotropy constant on the thickness of the main magnetic layer of the film in the range of 200–400 nm. The measurements were performed for the $Fe_{20}Ni_{80}$ composition. The second film series was synthesized with the Fe–Ni layer with a thickness of ~220 nm; a variable parameter was the nickel content (from 0 to 100 at %). In addition, the angular dependence of the FMR film was investigated.

The K_S value and spin-wave stiffness were measured by the SWR technique. The SWR spectra of the films were examined on a standard X-range spectrometer at a resonator pump frequency of $f = 9.2$ GHz at room temperature for the wave vectors of standing exchange spin waves from 10^5 to 2×10^6 cm^{-1}. The films were placed in an antinode of the ac magnetic field of a transmission-type resonator and magnetized along the surface normal.

The thickness and chemical composition of the layers of all the synthesized samples were controlled by X-ray spectral analysis on a DRON-4 diffractometer at a wavelength of $\lambda = 1.54056$ Å (CuK_α radiation).

3. SPIN-WAVE RESONANCE IN THIN FERROMAGNETIC FILMS

The spin-wave resonance is a phenomenon of resonance absorption of the rf field energy in a magnetic film with a thickness equal to the integer number of half-wavelengths of the exchange spin wave with the wave vector directed along the surface normal [24]. Let us consider such a situation in a film uniformly magnetized to saturation by external field H. Then, the equilibrium position of magnetization is expressed as [25, 26]

$$H_{\text{eff}} \sin\varphi\cos\varphi = H\sin(\varphi - \alpha_H), \qquad (2)$$

where φ is the angle between the normal to the film surface and the magnetization direction, α_H is the angle between the film normal and applied field H, and H_{eff} is the effective field taking into account the effect of anisotropy from different sources. In the case of a homogeneous isotropic film, we have $H_{\text{eff}} = 4\pi M_S$, where M_S is the saturation magnetization; in the general case, we have $H_{\text{eff}} = 4\pi M_{\text{eff}}$.

The uniform natural oscillations of the magnetization are described by the expression

$$\left(\frac{\omega_0}{\gamma}\right)^2 = (H\cos(\varphi - \alpha_H) - H_{\text{eff}}\cos 2\varphi) \times (H\cos(\varphi - \alpha_H) - H_{\text{eff}}\cos^2\varphi), \qquad (3)$$

where ω_0 is the frequency of uniform magnetization precession and γ is the gyromagnetic ratio.

The simultaneous solution of Eqs. (2) and (3) allows one to obtain the well-known Kittel formulas [27] for determining the resonance field of a platelike sample:

$$\left(\frac{\omega_0}{\gamma}\right)^2 = (H - H_{\text{eff}})^2 \quad (\text{at} \quad \alpha_H = 0°),$$
$$\left(\frac{\omega_0}{\gamma}\right)^2 = H(H + H_{\text{eff}}) \quad (\text{at} \quad \alpha_H = 90°). \qquad (4)$$

The uniform ac magnetic field h ($\mathbf{h} \perp \mathbf{H}$) with frequency ω can excite nonuniform forced magnetization oscillations, which are now described by the dispersion relation

$$\left(\frac{\omega_0}{\gamma}\right)^2 = \left(H\cos(\varphi - \alpha_H) - H_{\text{eff}}\cos 2\varphi + \frac{2A}{M_S}k^2\right) \times \left(H\cos(\varphi - \alpha_H) - H_{\text{eff}}\cos^2\varphi + \frac{2A}{M_S}k^2\right), \qquad (5)$$

where A is the exchange coupling constant and k is the wave vector parallel to the film normal, which is determined by the boundary conditions on the film surfaces.

Since, in the general case, surface spins are pinned differently on different film surfaces, the exchange boundary conditions are determined by the expressions [22, 23, 28]

$$\left(\frac{\partial \mathbf{m}}{\partial z} + \beta_1^S \mathbf{m}\right)_{z=L/2} = 0, \quad \left(\frac{\partial \mathbf{m}}{\partial z} - \beta_2^S \mathbf{m}\right)_{z=-L/2} = 0, \qquad (6)$$

where β_1^S and β_2^S are the parameters of pinning of the surface spins on different film surfaces, which is related to the surface anisotropy constant as $\beta^S = \frac{K_S}{A}$, and L is the film thickness.

Assuming the solution of Eq. (6) to be a plane wave and the pinning parameters on the upper and lower film surfaces to be arbitrary, we can determine the possible values of wave vector k from the expression

$$\tan(kL) = \frac{k\left(\frac{K_{S1}}{A} + \frac{K_{S2}}{A}\right)}{k^2 - \frac{K_{S1}}{A}\frac{K_{S2}}{A}}, \qquad (7)$$

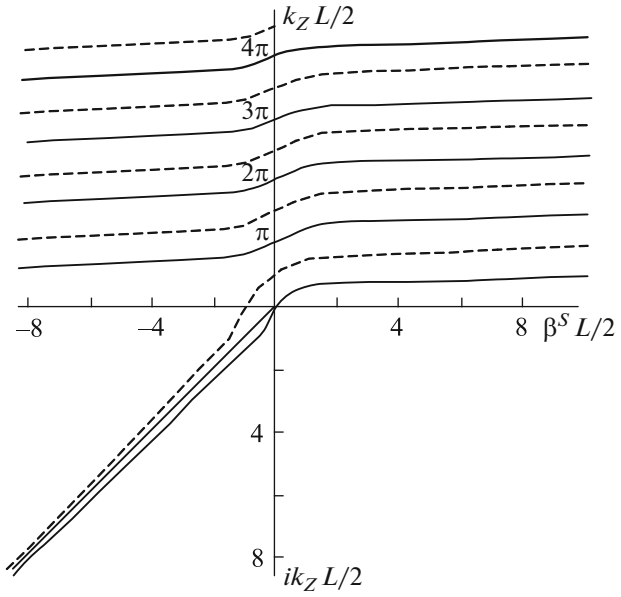

Fig. 1. Dependence of the wave vector k on the surface spin pinning parameter β^S for different SWR modes. Solid lines reflect the symmetric boundary conditions and dashed lines, the antisymmetric boundary conditions [28].

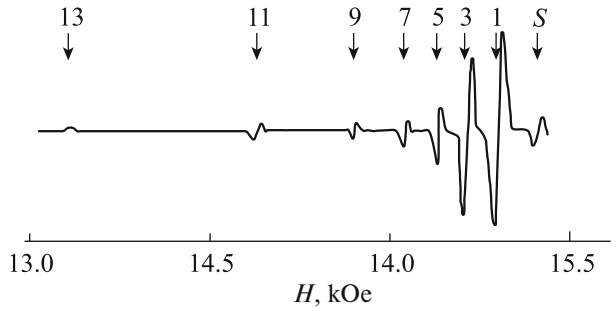

Fig. 2. SWR spectrum of the Co–Zr film; K_S = 0.055 erg/cm^2 at L = 270 nm [29].

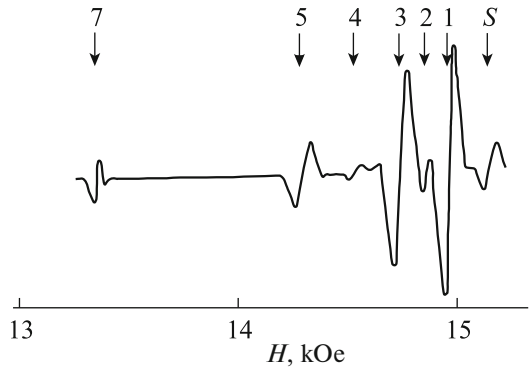

Fig. 3. SWR spectrum of the Fe–Zr film; K_S = 0.055 erg/cm^2 at L = 160 nm [30].

where K_{S1} and K_{S2} are the surface anisotropy constants on different film surfaces. The solution of this equation is plotted in Fig. 1.

The surface spin pinning parameter β^S and, consequently, the surface anisotropy constant K_S can take both positive and negative values (see Fig. 1). At $K_S > 0$ (the easy axis of the surface anisotropy is normal to the film plane), the harmonic SWR modes with the real vales of wave vector k are only excited. At $K_S < 0$ (the hard axis of the surface anisotropy is normal to the film surface), a hyperbolic nonpropagating exchange spin wave (surface mode) with the imaginary wave vector is detected in the SWR spectrum, along with the harmonic oscillations. At $K_S = 0$, the uniform ac magnetic field $h_\sim$ ($\mathbf{h} \perp \mathbf{H}$) only excites a uniform magnetization oscillation $\mathbf{m}_0 \perp \mathbf{M}$ (FMR), since all the rest possible oscillations $m(z)$ are characterized by zero dipole moment.

According to [15], under the symmetric boundary conditions with $K_S = \infty$, the allowed wave vector values are $k = \dfrac{\pi n}{L}$, where n is the number of the trigonometric mode (n = 1, 3, 5, 7, ...).

The shape of the SWR spectrum under the antisymmetric boundary conditions (the easy-axis pinning type on one surface and the easy-plane pinning type on the other surface) is determined by the ratio between the values $K_{S1} + K_{S2}$. The first possible variant is $|K_{S1}| = |K_{S2}|$, when the detected spectrum (see example in Fig. 2) shows the presence of one surface mode in the fields stronger than the field of the main trigonometric maximum and the absence of even modes. In the second variant, the $|K_{S1}|$ and $|K_{S2}|$ values strongly differ from one another (see example Fig. 3). In the third variant, the sum $K_{S1} + K_{S2}$ is slightly nonzero, which leads to the absence of the even mode with n = 2 in the spectrum (see example in Fig. 4). In addition, there can be a variant when the SWR spectrum contains two surface modes, which correspond to the conditions $K_{S1} < 0$ and $K_{S2} < 0$ (Fig. 5).

The pinning type is determined by the average magnetic moment on the surface, as well as by the magnetization distribution over the film thickness [32].

4. RESULTS AND DISCUSSION

The chemical deposition synthesis technique allowed us to obtain the films with $K_S < 0$, which led to the occurrence of a surface peak in the SWR spectra in field H_S stronger than field H_1 of the first trigonometric mode (Fig. 6).

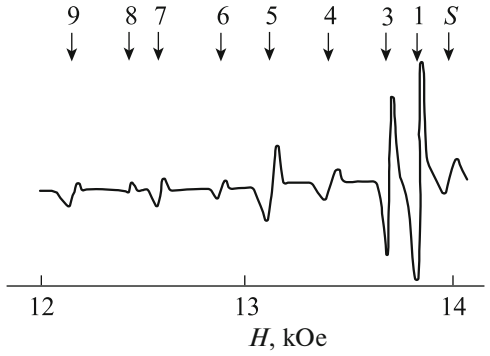

Fig. 4. SWR spectrum of the Co–P film; K_S = 0.144 erg/cm^2 at L = 170 nm [31].

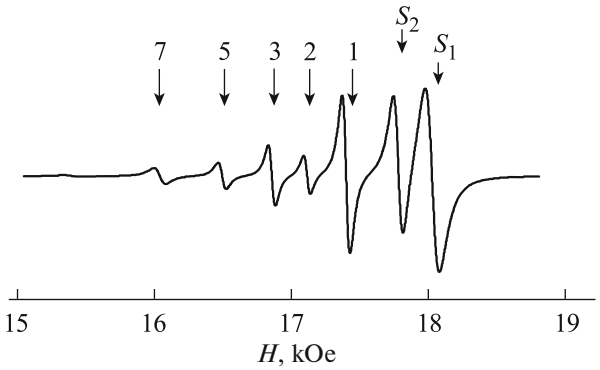

Fig. 5. SWR spectrum of the Fe–Ni film; K_S = 0.55 erg/cm^2 at L = 220 nm.

The expression for resonance fields at the perpendicular sample orientation ($\varphi = \alpha_H = 0$) in the external magnetic field with regard to Eq. (5) has the form

$$H_n = H_0 - \frac{2A}{M_S}k^2, \qquad (8)$$

where k is the wave vector, which, in our case, is related to the mode number n in the SWR spectrum by the simple relations $k = \frac{\pi}{L}n$ for the bulk spin-wave modes and $k = i\beta^S = i\frac{K_S}{A}$ for the surface mode; $H_0 = \frac{\omega}{\gamma} + 4\pi M_{\text{eff}}$ is the theoretical field of the uniform resonance ($n = 0$); and M_S is the saturation magnetization.

Expression (8) allows us to determine the spin-wave stiffness for the exchange spin waves from the experimental SWR spectrum

$$\eta = \frac{2A}{M_S} = \left(\frac{L}{\pi}\right)^2 \frac{H_n - H_{n+1}}{(n+1)^2 - n^2} \qquad (9)$$

in units of Oe cm^2 and, consequently, to calculate the exchange coupling constant $A = \eta M_S/2$ (erg/cm) and spin-wave stiffness in units of meV Å^2 ($D = \eta/g\mu_B$).

The surface anisotropy constant at $K_S < 0$ is calculated using the formula

$$|K_S| = \left[\frac{M_S A}{2}\left[(H_S - H_1) - \frac{2A}{M_S}\left(\frac{\pi}{L}\right)^2\right]\right]^{1/2}. \qquad (10)$$

Thus, the analysis of SWR spectra consists in the correct numeration of the detected modes and identification of the surface mode. According to [3, 18, 22, 23, 28, 33], the following numeration rules are used: the mode with $n = 0$ ($K_S = 0$) is only excited upon uniform magnetization precession; at the infinitely rigid pinning ($K_S \to \infty$) and symmetric (antisymmetric) boundary conditions, the odd modes are only reflected in the SWR spectrum; the even modes are excited at the finite $|K_S|$ values and nonzero dipole moment of the mode (the mode intensity is much lower than the odd mode intensity); the surface mode is observed in the spectrum at the implementation of the easy-plane boundary conditions ($K_S < 0$) on one (or both) film surface and is located in the spectrum in the fields stronger than the field of the first bulk mode.

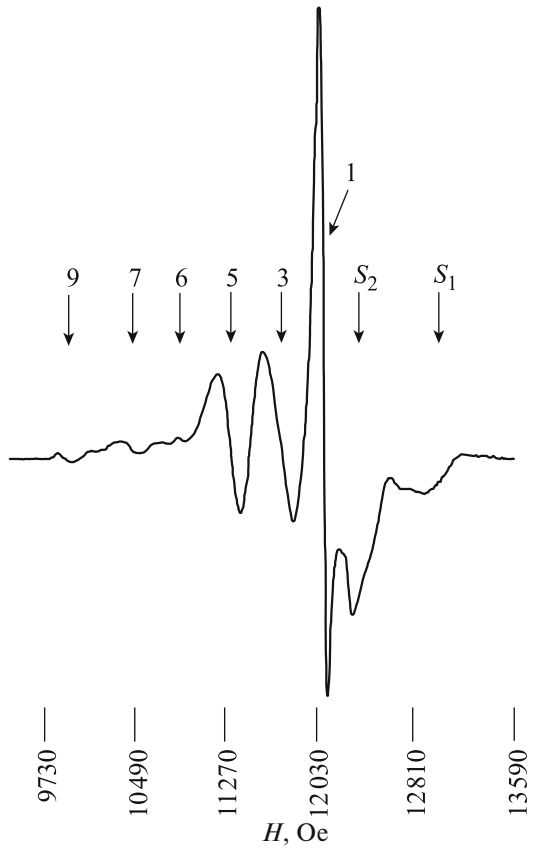

Fig. 6. SWR spectrum of the single-layer $Fe_{20}Ni_{80}$ film with a thickness of ~336 nm with the additional Co–P alloy layer.

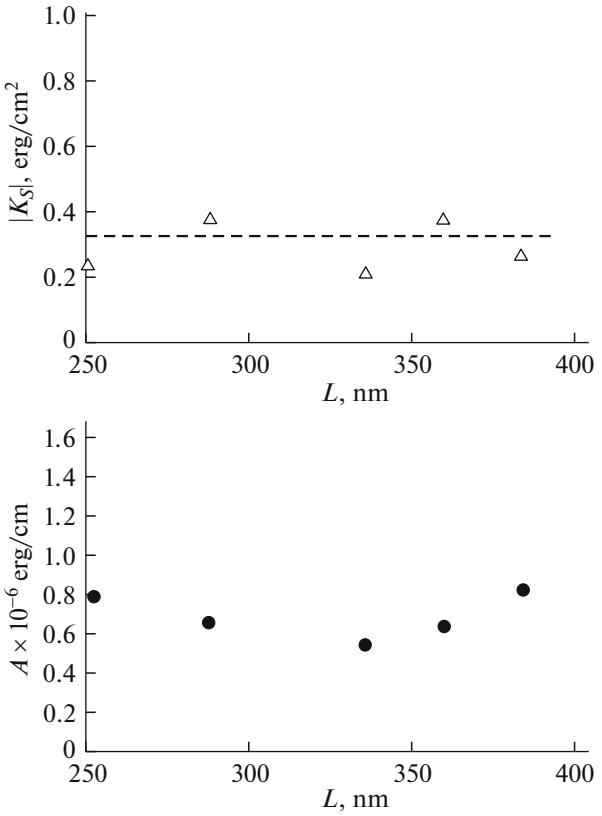

Fig. 7. Dependence of the $|K_S|$ and A values calculated, using formulas (10) and (9), respectively, on the Fe–Ni layer thickness.

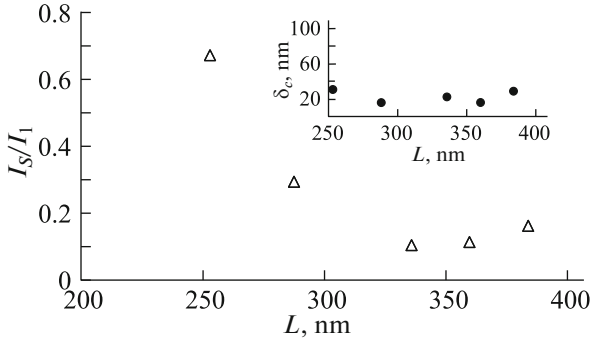

Fig. 8. Dependence of the ratio between intensities of the surface and first bulk mode and the surface mode penetration depth (inset) on the $Fe_{20}Ni_{80}$-layer thickness.

The detection of two surface modes simultaneously in the presented spectrum (Fig. 6) is indicative of K_{S1} and K_{S2} on the outer and inner film surfaces.

The errors in the spectrum interpretation can lead to the contradictory conclusions. In particular, the authors of [34] ignored the rule of the ratio between intensities of the even and odd modes during numerical simulation of the experimental SWR spectrum of the Co–Ni film, which led to the ambiguous values of the surface anisotropy constant.

In some cases, the conditions determining the ratio between intensities of the first bulk and surface modes are ignored; one of the most important conditions is the film thickness. The surface mode is described by the hyperbolic function of spatial coordinate z and characterized by the relative intensity and penetration depth $\delta_c \sim \frac{A}{K_S}$ [28]. According to the experimental data obtained in our work (Figs. 7 and 8), the δ_c value can be assumed to be constant upon film thickness variation within a certain range. The thickness dependences of the surface anisotropy and exchange coupling constants were studied for a series of single-layer $Fe_{20}Ni_{80}$ ferromagnetic thin films and, in contrast to [35], the $|K_S|$ value in this sample series was found to be constant upon variation in the thickness of the main magnetic layer (Fig. 7). The lower sensitivity of K_S to the thickness variation was obtained by changing the synthesis technique and formation of an additional Co–P layer.

The relative intensity of bulk modes can be analytically estimated using the expression [28]

$$I_n \sim \frac{\sin^2(k_n L/2)}{(k_n L/2)^2}\left[1+\frac{\sin(k_n L)}{k_n L}\right]^{-1} \qquad (11)$$

and the relative intensity of surface modes, using the expression

$$I_S \sim \frac{\sinh^2(k_S L/2)}{(k_S L/2)^2}\left[1+\frac{\sinh(k_S L)}{k_S L}\right]^{-1}. \qquad (12)$$

Analysis of the detected SWR spectra for our films allowed us to determine the ratio between intensities of the surface and first bulk modes as a function of film thickness (Fig. 8).

At the film thickness $L \gg \delta_c$ (for our films, this inequality is valid at ~150 nm and more), the intensity of the surface mode is lower than the intensity of the first bulk mode. However, a decrease in the film thickness leads to an increase in the ratio I_S/I_1, up to the predominance of the surface mode in the SWR spectrum over the first mode. In our opinion, the similar situation was implemented in [36], where the authors identified the maximum peak in the SWR spectrum of the ultrathin (50 nm) FePt film as a uniform resonance mode and the peak with the next intensity, as the first mode. This allowed the authors to calculate the spin-wave stiffness for the exchange spin waves using the formula analogous to Eq. (9). If the experimental spectrum is identified differently—as excitation of the surface and first bulk modes—then, the SWR spectrum is described by formula (10). It can be seen from (10) that the large difference between the experimental fields $H_S - H_1$ (in [36], $H_S - H_1 =$

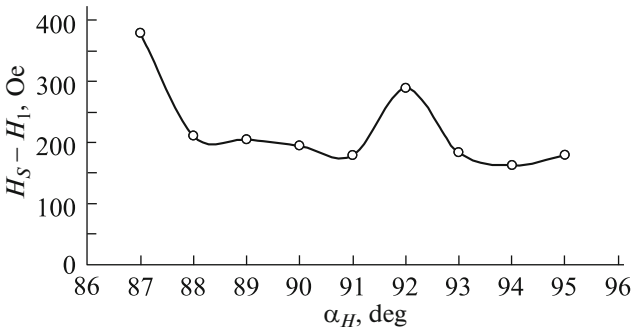

Fig. 9. Angular dependence of the field shift between the surface and first bulk modes.

1200 Oe) can be caused by both the $|K_S|$ value and $\frac{2A}{M_S}\left(\frac{\pi}{L}\right)^2$ value. Indeed, at $A = 0.95 \times 10^{-6}$ erg/cm and $M_S \approx 866$ G for the FePt films from [37], we obtain $\frac{2A}{M_S}\left(\frac{\pi}{L}\right)^2 \approx 865$ Oe; then, using Eq. (10), we can determine $|K_S| \approx 0.315$ erg/cm^2. The calculated surface anisotropy constant for the FePt films agrees well with the K_S values for the analogous films from [38], which were determined in this work using the Neel model.

Note that at the absence of the surface mode in the SWR spectrum ($K_S > 0$), the surface anisotropy constant can also be determined by the SWR technique. At the first stage, the angular dependence of the first bulk mode is measured; the data obtained together with Eqs. (2) and (5) allow the wave vector k to be determined. The next stage in the determination of the K_S value is substitution of the obtained result to Eq. (7). The methodological example of such an estimation of the K_S value was presented in [38].

The experimental angular dependence of $(H_S - H_1)$ measured on the $Fe_{20}Ni_{80}$ film with a thickness of $L \sim$ 336 nm (Fig. 9) makes it possible to estimate the degree and nonlinearity of the dependence of the wave vector on the external field direction. The critical angles at which the SWR spectrum stopped showing the surface mode peak (as well as the other peaks, except for the uniform resonance peak) are 84° and 95°; the angles of 87° and 92° correspond to the maximum difference between the surface and first mode. The character of the observed angular dependence can be caused by two sources. The first source is the interrelation between the wave vector and effective film thickness: the rotation of the film in the field by a certain angle leads to an increase in the effective thickness and, as a consequence, the change in the resonant field. The analytical calculation of such a behavior was predicted in [39].

The second source is the change in the effective conditions of surface pinning, which are determined by both the surface anisotropy energy and the magnetostatic energy formed by the difference between magnetizations in the bulk and on the surface of the film. The rotation of a sample in the external magnetic changes the contribution of the magnetostatic component, which can explain the maximum points in the angular dependences.

It is well known that the change in the alloy composition can facilitate structural transformations, which lead to the change in the magnetic parameters of a system. To study the effect of the alloy composition on the surface anisotropy constant, we measured the concentration dependence of this parameter. The films were fabricated at the main Fe–Ni magnetic layer thicknesses from 220 to 250 nm. The structural transformations that occur upon variation in the alloy composition were determined by X-ray diffraction analysis. The surface anisotropy constants were calculated from the SWR spectra of the films by formula (10). The normalized exchange stiffness $\left(\eta^* = \frac{2A}{M_S}\left(\frac{\pi}{L}\right)^2\right)$ in oersteds was determined using formula (9). These dependences are presented in Figs. 10 and 11.

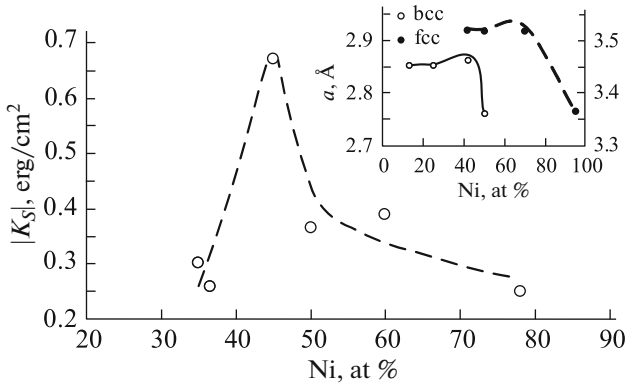

Fig. 10. Concentration dependences of the surface anisotropy constant and lattice constant (inset) for the Fe–Ni films.

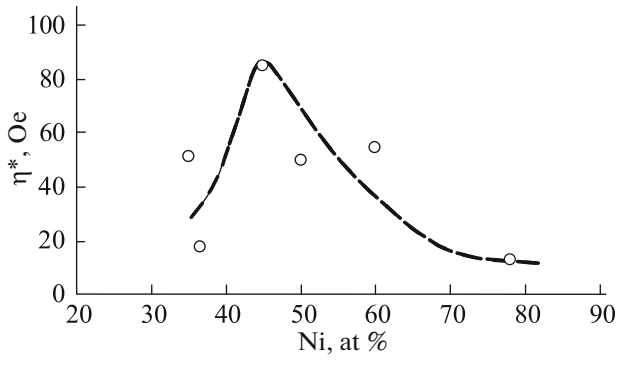

Fig. 11. Concentration dependences of the normalized exchange stiffness of the Fe–Ni films.

5. CONCLUSIONS

Thus, the results of SWR investigations of single-layer FeNi films demonstrate the possibilities of this technique both in estimating the pinning conditions and establishing the surface anisotropy constant and spin-wave stiffness.

The average $|K_S|$ value for a series of the $Fe_{20}Ni_{80}$ films (at the film thicknesses in the range of 250–400 nm) was about 0.34 erg/cm^2 and the exchange coupling constant, $A = (0.6–0.8) \times 10^{-6}$ erg/cm. The surface exchange spin penetration wave depth is $\delta_c =$ 20–30 nm.

The transformation of the atomic and nanostructure of the Fe–Ni films at the invar concentration ($x_c =$ 40–45 at %) is reflected on the concentration dependence of the exchange stiffness $\eta(x)$ near x_c and in the dependence of the surface anisotropy constant $K_S(x)$ in the same range of concentration x_c.

ACKNOWLEDGMENTS

This study was supported by the Russian Foundation for Basic Research, projects nos. 16-03-00256 and 16-03-00969.

REFERENCES

1. V. V. Kruglyak, C. S. Davies, V. S. Tkachenko, O. Yu. Gorobets, Yu. I. Gorobets, and A. N. Kuchko, J. Phys. D **50**, 094003 (2017).
2. A. I. Stognij, L. V. Lutsev, V. E. Bursian, and N. N. Novitskii, J. Appl. Phys. **118**, 023905 (2015).
3. R. S. Iskhakov, S. V. Stolyar, M. V. Chizhik, and L. A. Chekanova, JETP Lett. **94**, 301 (2011).
4. D. M. Jacobi, E. Sallica Leva, N. Alvarez, M. Vasquez Mansilla, J. Gomez, and A. Butera, J. Appl. Phys. **111**, 033911 (2012).
5. G. Thirupathi and R. Singh, AIP Conf. Proc. **1665**, 050133-1 (2015).
6. L. A. Chekanova, S. V. Komogortsev, E. A. Denisova, L. A. Kuzovnikova, I. V. Nemtsev, R. N. Yaroslavtsev, and R. S. Iskhakov, Bull. Russ. Acad. Sci.: Phys. **81**, 351 (2017).
7. L. Dreher, C. Bihler, E. Peiner, A. Waag, W. Schoch, W. Limmer, S. T. B. Goennenwein, and M. S. Brandt, Phys. Rev. B **87**, 224422 (2013).
8. A. I. Dmitriev, R. B. Morgunov, O. L. Kazakova, and J. Tanimoto, J. Exp. Theor. Phys. **108**, 985 (2009).
9. X. Liu and J. K. Furdyna, J. Phys.: Condens. Matter **18**, R245 (2006).
10. A. Butera, Phys. Rev. B **60**, 12270 (1999).
11. E. A. Denisova, S. V. Komogortsev, R. S. Iskhakov, L. A. Chekanova, A. D. Balaev, Y. E. Kalinin, and A. V. Sitnikov, J. Magn. Magn. Mater. **440**, 221 (2017).
12. D. A. Balaev, A. A. Krasikov, A. A. Dubrovskiy, S. I. Popkov, S. V. Stolyar, O. A. Bayukov, R. S. Iskhakov, V. P. Ladygina, and R. N. Yaroslavtsev, J. Magn. Magn. Mater. **410**, 171 (2016).
13. S. V. Stolyar, R. N. Yaroslavtsev, R. S. Iskhakov, O. A. Bayukov, D. A. Balaev, A. A. Dubrovskii, A. A. Krasikov, V. P. Ladygina, A. M. Vorotynov, and M. N. Volochaev, Phys. Solid State **59**, 555 (2017).
14. W. S. Ament and G. T. Rado, Phys. Rev. **97**, 1558 (1955).
15. C. Kittel, Phys. Rev. **110**, 1295 (1958).
16. A. V. Davydenko, A. G. Kozlov, A. V. Ognev, M. E. Stebliy, A. S. Samardak, K. S. Ermakov, A. G. Kolesnikov, and L. A. Chebotkevich, Phys. Rev. B **95**, 064430 (2017).
17. A. Stankov, in *Physics of Magnetic Films,* Ed. by V. A. Buravikhin (Vost.-Sib. Pravda, Irkutsk, 1968), p. 422 [in Russian].
18. V. M. Sokolov and B. A. Tavger, Sov. Phys. Solid State **10**, 1412 (1968).
19. H. Puszkarski, Acta Phys. Polon. A **38**, 217 (1970).
20. H. Puszkarski, Phys. Status Solidi A **38**, 145 (1970).
21. B. N. Filippov, Fiz. Met. Metalloved. **32**, 911 (1971).
22. Yu. A. Korchagin, R. G. Khlebopros, and N. S. Chistyakov, Sov. Phys. Solid State **14**, 1826 (1971).
23. Yu. A. Korchagin, R. G. Khlebopros, and N. S. Chistyakov, Fiz. Met. Metalloved. **34**, 1303 (1972).
24. *Magnetism and Magnetic Materials, Terminological Handbook,* Ed. by F. V. Lisovskii and L. I. Antonov (VAGRIUS, Moscow, 1997) [in Russian].
25. A. G. Gurevich and G. A. Melkov, *Magnetization Oscillations and Waves* (CRC, Boca Raton, 1996).
26. M. Farle, Rep. Prog. Phys. **61**, 755 (1998).
27. C. Kittel, Phys. Rev. **73**, 155 (1948).
28. N. M. Salanskii and M. Sh. Erukhimov, *Physical Properties and Application of Magnetic Films* (Nauka, Novosibirsk, 1975) [in Russian].
29. R. S. Iskhakov, M. M. Brushtunov, and A. S. Chekanov, Sov. Phys. Solid State **29**, 1553 (1987).
30. R. S. Iskhakov, M. M. Brushtunov, A. G. Narmonev, I. A. Turpanov, and L. A. Chekanova, Fiz. Met. Metalloved. **79** (5), 122 (1995).
31. V. A. Ignatchenko, R. S. Iskhakov, L. A. Chekanova, and N. S. Chistyakov, Sov. Phys. JETP **48**, 328 (1978).
32. J. T. Yu, R. A. Turk, and P. E. Wigen, Phys. Rev. B **11**, 420 (1975).
33. A. G. Gurevich, *Magnetic Resonance in Ferrites and Antiferromagnets* (Nauka, Moscow, 1973) [in Russian].
34. P. Talagala, P. S. Fodor, D. Haddad, R. Naik, L. E. Wenger, P. P. Vaishnava, and V. M. Naik, Phys. Rev. B **66**, 144426 (2002).
35. I. G. Vazhenina, L. A. Chekanova, and R. S. Iskhakov, Bull. Russ. Acad. Sci.: Phys. **81**, 308 (2017).
36. C. Antoniak, J. Lindner, K. Fauth, J.-U. Thiele, J. Minár, S. Mankovsky, H. Ebert, H. Wende, and M. Farle, Phys. Rev. B **82**, 064403 (2010).
37. E. Sallica Leva, R. C. Valente, F. Martınez, M. Vasquez Mansilla, S. Roshdestwensky, and A. Butera, Phys. Rev. B **82**, 144410 (2010).
38. E. Burgos, E. Sallica Leva, J. Gomez, F. Martınez Tabares, M. Vasquez Mansilla, and A. Butera, Phys. Rev. B **83**, 174417 (2011).
39. P. E. Wigen, C. F. Kooi, M. R. Shanabarger, and Th. D. Rossing, Phys. Rev. Lett. **9**, 206 (1962).

Translated by E. Bondareva